Biochemical and Biophysical Research Communications 455 (2014) 198–204

Contents lists available at ScienceDirect

Biochemical and Biophysical Research Communications

journal homepage: www.elsevier.com/locate/ybbrc

An alternative method of enhancing the expression level of heterologous protein in *Escherichia coli*

Jun Yin [1], Hong Tian [1], Lichen Bao, Xin Dai, Xiangdong Gao *[,2], Wenbing Yao *

State Key Laboratory of Natural Medicines, School of Life Science and Technology, China Pharmaceutical University, Nanjing 210009, China

ARTICLE INFO

Article history:
Received 23 October 2014
Available online 5 November 2014

Keywords:
Expression level
Translation initiation region
mRNA secondary structure
ΔG
Translation efficiency

ABSTRACT

Though numerous strategy options are available for achieving high expression levels of genes in *Escherichia coli*, not every gene can be efficiently expressed in this organism. By investigating the relationship between the mRNA secondary structure of translational initiation region (TIR) and gene expression in *E. coli*, we establish a simple method to design sequences of appropriate TIR (from −35 to +36) that meet a specific expression level as we need. Using this method, overexpression of native human humor necrosis factor α and extracellular domain of Her2/neu protein (aa 23–146) in *E. coli* were achieved. Differences in expression appeared was mainly related to the efficiency of translation initiation and the stability of mRNA secondary structure, because the intracellular mRNA levels analyzed by real-time RT-PCR were quite similar. Our approach can overcome the steric hindrance of translation startup, and therefore promote translation smoothly to acquire high expression of exogenous protein.

1. Introduction

The expression of target protein in different hosts is unpredictable and challengeable. It can be affected by various factors, including the copy number and stability of the expression plasmid, the feature of target gene, the synthetic level and stability of mRNA, the structure and stability of the synthesized protein [1–3]. Many advantages of *Escherichia coli* have ensured that it remains a very valuable organism for the high-level production of recombinant proteins [4,5]. Despite the substantial knowledge on the genetics and molecular biology of *E. coli*, it is still difficult to express every gene efficiently in this organism [6]. In addition, no gold criteria have been established in *E. coli*, and strategies for the optimization of expression level differ greatly from gene to gene and are often decided by trial and error.

In the previous study, the native human tumor necrosis factor α (TNF-α) presents poor expression level in some strong prokaryotic expression vectors, even in pET vectors. After fused a His_6-Tag to the N terminal of human TNF-α gene, the expression of this protein was remarkably enhanced. The unique difference between the native TNF-α and His_6-TNF-α is the His_6-Tag which contains continuous 6 CAU codons just next to the initiation AUG codon. We considered that the remarkable increase of the expression level may be correlated to the enlargement of A/U base-pair ratio in translational initiation region (TIR). To enhance the expression of exogenous protein without changing the amino acid sequence, we focus on the relationship between the TIR and gene expression.

It is now clear that the various translation efficiencies of different mRNAs are predominantly due to the unique structural features at the 5′ end of each mRNA [7–9]. Meanwhile, the mRNA secondary structure of translation initiation region (TIR) plays a crucial role in the efficiency of gene expression [10–12]. The stability of mRNA secondary structure is quantified as the value of minimal folding free energy (ΔG). An increase in the ΔG of 1.4 kcal/mol corresponds to the reduction by a factor of 10 in translation initiation rate [13]. Wu et al. used ΔG of the secondary structure as the index and chose a 73 bp fragment of TIR from +1 to +73, optimized the TIR of xylanase gene from *Thermotoga maritima*. Consequently, the xylanase was successfully overexpressed in *E. coli* [14]. In particular, Seo et al. found the ΔG of the downstream region (DR) was linearly associated with the relative expression level over a range of 4-fold change in *E. coli* [15]. Though the ΔG of TIR is found to be correlated with the relative expression level, there has been no straightforward approach that can direct us about how to design sequences of TIR that meet a specific expression level as we need.

In this study, we seek to establish a universal method that could regulate the expression level of target protein without changing

* Corresponding authors. Fax: +86 25 83271249 (X. Gao). Fax: +86 25 83302827 (W. Yao).
E-mail addresses: xdgao@cpu.edu.cn (X. Gao), wbyao@cpu.edu.cn (W. Yao).
[1] These authors contributed equally to this work.
[2] We designate this one to further communicate with the Editorial and Production offices.

http://dx.doi.org/10.1016/j.bbrc.2014.10.149
0006-291X/

the amino acid sequence by optimizing the mRNA secondary structure of TIR. Based on this method, we further develop a general tool, called OpTIR. Silent mutations were systematically introduced into specific codons at the 5′ end of exogenous gene to modulate the local secondary structure of the mRNA, recombined with the same vector to form different TIRs after optimization. By these results, we may get a series of sequences, which contain some specific expression levels as we need. Furthermore, we report the significant improvement of the expression levels of human TNF-α and Her2 (aa 23–146) in *E. coli* by using our method. Extracellular domain of Her2/neu protein (aa 23–146) containing two Her2 T-helper epitopes: p42 (aa 42–56), p98 (aa 98–114) [16] is likely to be chosen for an anti-Her2 vaccine to break the immunological tolerance. Thereby, we can optimize the gene sequence at the beginning phase of recombinant protein expression to avoid repeatedly designing the target gene from scratch for high expression.

2. Materials and methods

2.1. Bacterial strains, plasmids and biochemical reagents

E. coli DH5α, *E. coli* BL21(DE3) and pET28a(+) vector were purchased from Invitrogen. Human TNF-α gene (GenBank NO. KM658597) and Her2 (aa 23–146) gene (GenBank NO. KM658598) were synthesized by Invitrogen (Shanghai, China). *E. coli* DH5α was used for cloning and amplifying plasmids and *E. coli* BL21 (DE3) was employed for expression. PrimerStar DNA polymerase and LA Taq DNA polymerase (Takara, China) were used for PCR. Restriction enzymes and goat anti-rabbit IgG conjugated alkaline phosphatase were purchased from Sangon Biotech (Shanghai) Co., Ltd. (China). Primers were synthesized by Invitrogen Corporation Shanghai Representative Office (China). For immunoblot analysis, rabbit anti-human TNF-α antibody was obtained from Anbo Biotechnology Co., Ltd. (USA).

Table 1
The appropriate codons for coding the 2–12th amino acids of target protein.

Amino acid	Codon	Amino acid	Codon
F	UUU UUC	H	CAU CAC
L	UUA UUG CUU CUG	Q	CAA CAG
I	AUU AUC	N	AAU AAC
M	AUG	K	AAA AAG
V	GUU GUC GUA GUG	D	GAU GAC
S	UCU AGC AGU	E	GAA GAG
P	CCU CCA CCG	C	UGU UGC
T	ACU ACC ACA ACG	W	UGG
A	GCU GCC GCA GCG	R	CGU CGC
Y	UAU UAC	G	GGU GGC GGG

2.2. Tool development based on ΔG of mRNA TIR

According to *E. coli* codon preference, we removed a portion of non-preference codons that are less frequently used so that the appropriate codons could be chosen to code the 2–12th amino acids of target protein (Table 1). Then, all possible combinations of mRNA sequences coding 2–12th amino acids of the target protein were calculated, recombined with the 35 bases upstream of the start codon in the vector and initiator codon AUG to form the various TIRs. We used ViennaRNA Package [17] to calculate ΔG of these TIRs, arraying the order based on their ΔG value. This tool provided the number of outputs depended on the index value of ΔG we set, making us easier to choose the ΔG that interested us for encoding the target protein in *E. coli*. The optimization of gene sequence mentioned above was achieved by using C language on Linux system (Online Resource 1). The calculation process was developed into a general tool named OpTIR (Fig. 1A).

2.3. Molecular cloning

DNA digestion and molecular cloning were performed following standard procedures [18], and DNA restriction and modification enzymes were purchased from Takara. Plasmids or DNA fragments were isolated from *E. coli* cells or agarose gels with TIANprep Mini Plasmid Kid, or TIANgel Midi Purification Kit, respectively.

2.4. RNA secondary structure prediction and gene mutagenesis

The secondary structures of mRNA in the TIRs of human TNF-α and Her2 (aa 23–146) were predicted using the algorithm of minimum free energy by online Vienna RNA Secondary Structure Prediction program (http://rna.tbi.univie.ac.at/cgi-bin/RNAfold.cgi). The selected regions for predicting were defined from the point −35 to +36 including the Shine-Dalgarno (SD) and the transcription start

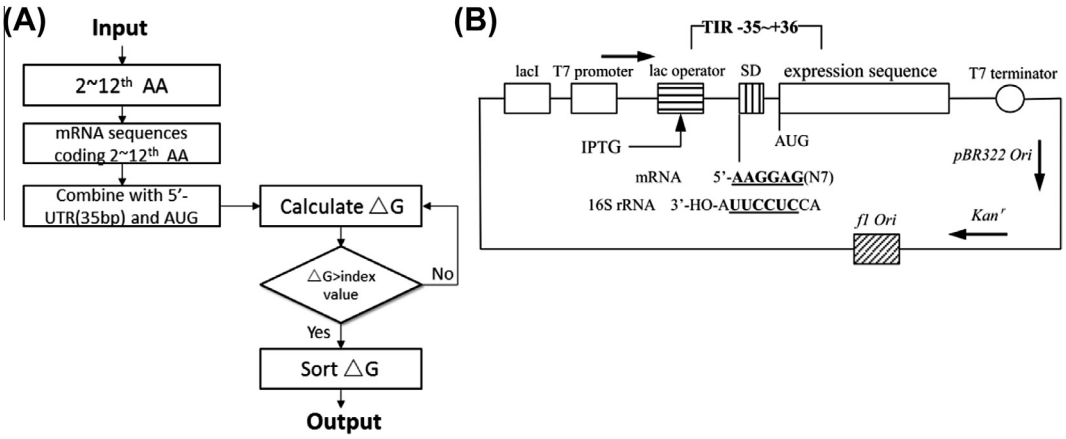

Fig. 1. (A) Schematic representation of the calculation process for the tool named OpTIR. (B) Schematic presentation of the features and sequence elements of the prokaryotic expression vector pET28a(+). The direction of transcription is indicated by the bold arrow. The part of TIR (from −35 to +36) consists of the SD sequence followed by an A+T-rich translational spacer that has an optimal length of approximately 7 bases. As shown, the 3′ end of the 16S rRNA interacts with the SD sequence during translational initiation. The repressor is encoded by a regulatory gene (lacI), which may suppress the activity of the lac operator. The activity of the lac operator is induced by the isopropylthiogalactoside (IPTG). The expression region of coding strand is transcribed by T7 RNA polymerase on account of T7 promoter. The transcription T7 terminator serves to stabilize the mRNA and the vector. In addition, an antibiotic resistance gene for kanamycin facilitates phenotypic selection of the vector, and the origin of replication (ori) determines the copy number of the vector. The various features are not drawn to scale.

site (TSS) in pET28a-hTNF-α and pET28a-Her2. According to the OpTIR analysis, the mutagenic oligonucleotides (5′-ATGGTGCGTTC TAGTTCTCGTACCCCGTCTGATAAA-3′, 5′-ATGGTTCGTTCTAGTTCTC GTACCCCGTCTGATAAA-3′) and (5′-ATGACCCAAGTTTGCACCGG TACCG ATATGAAATTA-3′) were designed to reduce the local second structures of mRNA. The mutant TNF-α and Her2 genes were cloned in frame within *Nco* I and *Hin*dIII restriction sites of the pET28a expression vector. All constructs were maintained in *E. coli* DH5α with kanamycin as selection pressure for subsequent expression in *E. coli* BL21 (DE3).

2.5. Real-time PCR analysis

For quantitative RT-PCR analyses, total RNA was extracted from the same cell culture which was utilized to analyze the protein expression. Total RNA was isolated from the cell pellet by using EasyPure™ RNA Kit (Transgen, China) and cDNA was synthesized using GoTaq® 2-Step RT qPCR System (Promega, USA). The primer pairs used for Q-PCR assays were TNF-α forward, 5′- CCGT CTGAAGGCCTGTATCT-3′, and TNF-α reverse, 5′- CAGCACATGGG TACTTGGAC-3′; and Her2 forward, 5′- TCAGGAAGTGCAAGGCTATG -3′, and Her2 reverse, 5′- TGGTATTATTCAGCGGATCG-3′; and 16s rRNA forward, 5′-CATGCCGCGTGTATGAAGAA-3′, and 16s rRNA reverse, 5′- CGGGTAACGTCAATGAGCAAA-3′. The quantitative RT-PCR was performed by using SYB green (Applied biosystem, USA) according to the manufacturer's instructions (Stepone plus, Applied biosystem). The mRNA expression of TNF-α and Her2 was normalized to the level of 16s rRNA mRNA.

2.6. Expression of recombinant proteins

The recombinant strains were cultured in LB medium containing 100 μg/mL kanamycin, and the cells were grown at 37 °C and 220 rpm until OD_{600} reached to 0.8–1.0. The cultures were further incubated with isopropyl-β-d-thiogalactoside (IPTG) at a final concentration of 1 mM, and cells were grown at 37 °C for additional 4 h. The uninduced samples were cultured under the same conditions except without the additional IPTG. 15% sodium dodecyl sulfate polyacrylamide gel electrophoresis (SDS–PAGE) and Western blot were used for analyzing the expression levels of the TNF-α and Her2 (aa 23–146). The Western blotting was carried out with a rabbit anti-human TNF-α antibody (1:10,000 dilutions) as primary antibody and horseradish peroxidase-conjugated goat anti-rabbit Ig antibody (1:5000 dilutions) as secondary antibody for detection of TNF-α. Expression levels were calculated by densitometric scanning of Coomassie-stained SDS-gels.

3. Results

3.1. OpTIR-driven optimization of mRNA TIR

One of the many expression systems tested is pET28a, a member of quite useful, well regulated and efficient vectors for heterologous gene expression in *E. coli*. The construction of an expression plasmid requires some elements whose configuration must be cautiously considered to ensure the highest level of protein synthesis [6,19,20]. The essential architecture of pET28a and the region of TIR (from −35 to +36) are shown in Fig. 1B. Despite its strong transcription and translation regulation signals, human TNF-α and Her2 (aa 23–146) were still poorly expressed with the optimized codon usage and sequence.

Based on ViennaRNA Package, we developed a general tool named OpTIR to search the optimal Δ*G* by designing mRNA TIR sequence that covers a desired range of Δ*G*. Each optimized sequence is changed with little mutations on its sequence; while its Δ*G* is dramatically increased. If the Δ*G* is found to be correlated with the relative expression level, we can also find a sequence in the output that meets a specific expression level as we need.

The Δ*G* of mRNA TIR from the points −35 to +36 in pET28a-hTNF-α was predicted by OpTIR (Table 2). The Δ*G* of the wild-type was −10.40 kcal/mol, while the range of Δ*G* values that we predicted was from −10.40 to −5.40 kcal/mol. To verify whether the Δ*G* of these results are closely related to the expression level, we picked up 3 genes from the output, wild-type, 1 and 6, correspond to wild-type, the intermediate product and the optimal mutation, respectively. Multiple nucleotides of these three genes that we picked were altered by site-directed mutagenesis (Fig. 2) based on the increased Δ*G*. The secondary structure of TIR of pET28a-TNF-α predicted by online Vienna RNA Secondary Structure Prediction program is depicted in Fig. 2. First, we mutate four nucleotides in TIR without changing the amino acid sequence and Δ*G* is moderately raised (Fig. 2B). Then, after the stepwise silent mutation, the hairpin structure of TIR is simplified significantly, and Δ*G* is elevated to −5.40 kcal/mol (Fig. 2C). In the meantime, the occlusion of the initiation codon AUG by a stem-loop structure appeared during the optimization process (Fig. 2C). According to the theory, this optimization can largely avoid the block of 30S ribosomal subunit binding to mRNA [21], promoting translation smoothly to acquire high expression of target protein. In order to verify the feasibility of the OpTIR tool in vivo, another protein, Her2 (aa 23–146), is selected for achieving high expression level simultaneously. Fig. 2 also shows the predicted secondary structure of TIRs by online Vienna program, including the wild-type of Her2 (Fig. 2D) and the optimal mutation based on the OpTIR tool (Fig. 2E), and the position where the mutations were introduced. In comparison between the wild-type and the optimal mutation, Δ*G* is increased from −10.30 to −4.00 kcal/mol.

3.2. Increased the expression level significantly driven by OpTIR tool

During this study, a series of expression plasmids were built, including the wild-types and variants. These expression plasmids were transformed into *E. coli* BL21 (DE3) competent cells respectively. The results of SDS–PAGE and Western blot show that each strain has a band of target molecular about 17KDa TNF-α protein before or after optimization (Fig. 3A and B). The expression level of the first mutated human TNF-α is only moderately increased. However, the final optimization of the target gene with much higher Δ*G* has obvious advantages on the expression level. By ana-

Table 2
The output of OpTIR. Silent mutations introduced in the mRNA TIR of pET28a-TNF-α.

Mutant[a]	Sequence[b]	Δ*G* (kcal/mol)
Wild-type	AAUAAUUUUGUUUAACUUUAAGAAGGAGAUAUACC	−10.40
1	**AUG**GUGCGUAGCAGCUCUCGUACCCCGUCUGAUAAA AAUAAUUUUGUUUAACUUUAAGAAGGAGAUAUACC	−10.00
2	**AUG**GUGCGUUCUAGUUCUCGUACCCCGUCUGAUAAA AAUAAUUUUGUUUAACUUUAAGAAGGAGAUAUACC	−9.00
3	**AUG**GUUCGUAGUUCUAGCCGUACGCCGAGUGACAAA AAUAAUUUUGUUUAACUUUAAGAAGGAGAUAUACC	−8.00
4	**AUG**GUGCGCAGCAGCUCUCGUACACCUAGUGAUAAG AAUAAUUUUGUUUAACUUUAAGAAGGAGAUAUACC	−7.00
5	**AUG**GUCCGUAGCAGCAGCCGUACGCCGAGUGAUAAA AAUAAUUUUGUUUAACUUUAAGAAGGAGAUAUACC	−6.00
6	**AUG**GUCCGCAGUAGUAGCCGCACCCCGAGCGACAAG AAUAAUUUUGUUUAACUUUAAGAAGGAGAUAUACC	−5.40
	AUGGUUCGUUCUAGUUCUCGUACCCCGUCUGAUAAA	

[a] An excerpt from the output is listed.
[b] Underlined and bold sequences represent the initiation codon.

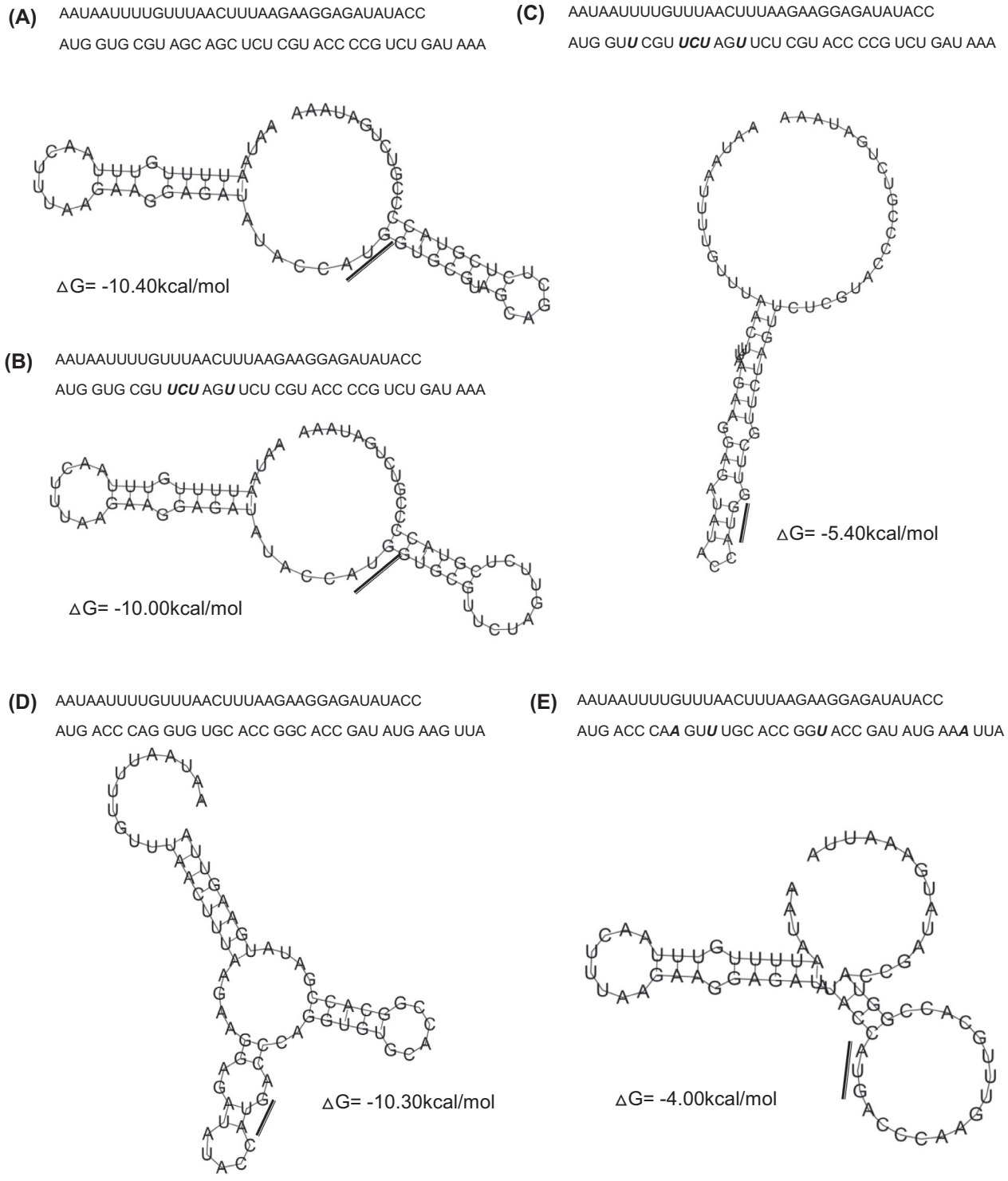

Fig. 2. The nucleotide sequences and secondary structures in TIRs (from −35 to +36) (numbering, +1 the translational initiation site) of pET28a-TNF-α and pET28a-Her2 (aa 23–146). Bold and italic nucleotides were mutated without changing the amino acid sequence. The mRNA secondary structure and Δ*G* of TIR for (A) wild-type of TNF-α, (B) the intermediate product of TNF-α, (C) the optimal mutation of TNF-α, (D) wild-type of Her2 and (E) the optimal mutation of Her2 predicted using Vienna RNA Secondary Structure Prediction program (http://rna.tbi.univie.ac.at/cgi-bin/RNAfold.cgi). The start codons marked by underline is shown in the structure illustrations.

lyzing the gel electrophoresis quantitatively (Fig. 3C), the result shows the expression level of the target protein has a fourfold increase after the optimization, which is even slightly higher than His_6-TNF-α. Furthermore, the recombinant expression of the optimal Her2 variant was nearly 4-fold greater than the wild-type in *E. coli* using the pET28a vector (Fig. 3D). Densitometric scanning of each corresponding bands measured by Quantity One® (Bio-Rad), 57.7% of total host cellular protein was achieved from the optimal Her2 mutation (Fig. 3E). Consequently, the optimization of mRNA secondary structure can significantly increase the expression level of the target protein to reveal that the OpTIR tool is simple and efficient.

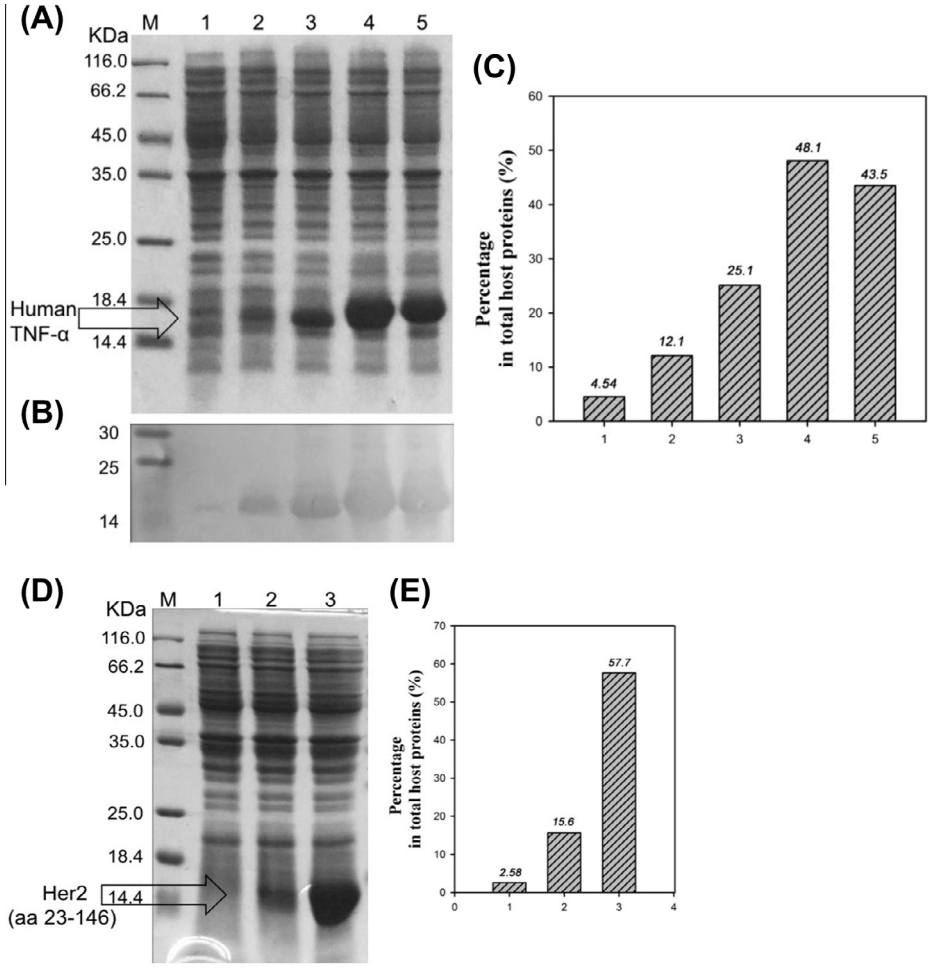

Fig. 3. Expression of the native and mutated proteins. (A) Human TNF-α induced by IPTG in *E. coli* BL21 (DE3). SDS–PAGE (15%), protein bands were stained with coomassie brilliant blue R250 reagent. M = molecular weight marker, Lane 1: uninduced bacterial lysate, Lane 2, 3, 4, and 5: IPTG induced bacterial lysate with native human TNF-α, the intermediate product, the optimal mutation and His-TNF-α. (B) The products are the TNF-α protein, as confirmed by Western blot with a rabbit anti-human TNF-α antibody. (C) SDS–PAGE quantitative analysis of Fig. 3A by Quantity One® (Bio-Rad). (D) Her2 (aa 23–146) induced by IPTG in *E. coli* BL21 (DE3). SDS–PAGE (15%), protein bands were stained with coomassie brilliant blue R250 reagent. M = molecular weight marker, Lane 1: uninduced bacterial lysate, Lane 2 and 3: IPTG induced bacterial lysate with wild-type and the optimal mutation. (E) SDS–PAGE quantitative analysis of Fig. 3D by Quantity One® (Bio-Rad).

3.3. Optimizations of mRNA secondary structure have no effect on mRNA level in E. coli

When the translation begins, ribosomes will bind to the 5′ end of the growing mRNA before the synthesis of the mRNA is completed in prokaryocytes, so the alteration of transcription status also impacts on its expression level. In order to verify whether the alteration of mRNA secondary structure had a marked impact on the transcription level of exogenous gene, the levels of mRNA were determined in each case by real-time PCR. The analysis revealed no significant differences in mRNA between wild-types and mutations of TNF-α and Her2, although remarkable differences in their expression levels were observed (Fig. 4).

4. Discussion

According to reports, until now, there has been no clearly defined specific range of TIR. The ribosome binding site (RBS), defined as the segment of mRNA protected against RNase digestion, consists of ~15 bp on each side of the initiation codon [22]. Nowadays, some researches of mRNA secondary structure are based mainly on the downstream region of initiation codon [23,24]. Nonetheless, Park et al. described the translation efficiency was affected by the ribosome binding affinity and its accessibility that is mainly dependent on the mRNA secondary structure in the 5′-untranslated region (UTR) [25]. As well, we consider the TIR should include the complete region of RBS not just the 5′ end of the coding region [26]. In addition, we should also ensure that there are sufficient nucleotides at the both sides of RBS, so that the conceivable local secondary structure of TIR could be formed. Hence, in my opinion, it is most reasonable that the optimization of mRNA secondary structure is based on the region of TIR from the points −35 to +36.

In this study, we focus on comparing the expression levels among a series of different sequences in the TIR with different secondary structures under the same expression systems and conditions. Since no 5′ exonuclease has been identified to date in prokaryotes [27], and the 3′ termini of TNF-α and Her2 genes have not been changed after the mutation, meanwhile 3′ exonucleolytic initiation of RNA decay is probably rare [28], we could reason out the alteration of mRNA secondary structure of TIR does not cause the change of transcriptional level. The Q-PCR results appear to validate our assumption that their mRNA levels should be no different after the mutation in the TIR. Hence, the reason of the increasing of expression level is tightly related to translational regulation.

The mRNA secondary structure is optimized from −35 to +36 of TIR to reduce the formation of hairpin structures considerably and

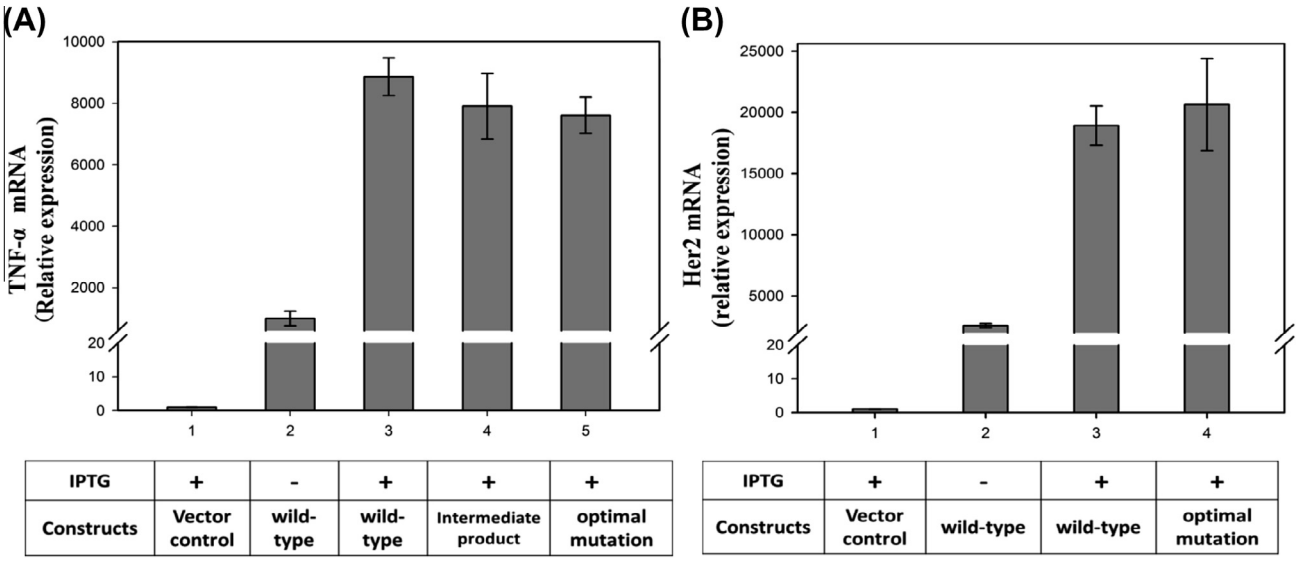

Fig. 4. Optimizations of mRNA secondary structure have no effect on mRNA level in *E. coli*. A and B show the results of Quantitative RT-PCR of the expression of mRNA encoding TNF-α and Her2 induced with/without IPTG. Values are normalized to their average 16s rRNA values and are presented as relative expression units. The BL21 strain transformed with empty vector was used as vector controls as indicated in all the experiments. Error bars indicate ± SD among duplicate samples from one experiment. Data are representative of three independent experiments with similar results.

the ΔG is elevated significantly. Collectively, the stability of the mRNA secondary structure around the initiation codon predominantly affected the translation efficiency. Zhang et al. demonstrated that exposure of the initiator codon AUG from local secondary structure at 5′- end of mRNA may be used as a general strategy for exogenous protein production in *E. coli* [29]. But, we find no evidence that exposure of only the SD region or the start codon preferentially favors translation. The results only reveal that the ΔG of TIR may have close relations to expression level, and whether the location of the start codon AUG and the SD region in or not in the stem-loop structure seems not to be the major factor. In order to make our method simple, we only emphasize the ΔG value regardless of the location of the initiation codon and the SD region in this method.

In this report, we indicate a universal method to regulate the expression level of exogenous protein in *E. coli* for the first time. First of all, we need to ascertain an appropriate region of TIR (from −35 to +36). Then, the ΔG of TIR could be chosen as a straightforward and visual index to evaluate the expression level of exogenous protein. Secondly, the content of A/U base pairs around the region downstream of the initiation codon is augmented by codon degeneracy. Simultaneously, we make sure that there will not be rare codons in *E. coli* caused by mutations in the coding region of TIR. In that case, to stepwise mutate G/C pair into A/U pair, ΔG could be increased significantly and effortlessly. As a result, the significant increase of ΔG means the decrease of mRNA secondary structure in TIR which leads to the improvement of the expression level of exogenous protein in *E. coli*.

In view of the above-mentioned method and based on ViennaRNA Package, we developed a general tool named OpTIR to guide the expression of exogenous protein in *E. coli* in a quick and intuitive manner. We then applied this tool to Her2 (aa 23–146) as well and significantly improved its expression level which demonstrated the feasibility of this approach in addition to the close relationship between ΔG of TIR and the expression level. In this study, we use only one vector, pET28a. Actually this tool is suitable for all prokaryotic expression vectors just by replacing the 35 bases upstream of the initiation codon in the vector.

It is noticeable that although we focused on the improvement of expression level while neglecting properties of the exogenous protein and other effects, inevitably bringing difficulties into application, clarifying relationship between secondary structure of mRNA and the expression level is still instructive. Increasing the ΔG of the adjacent area of RBS within appropriate ranges promises to increase the expression level exponentially. When the improvement reaches a limit, it will enter a platform, while all the other effects dominate.

Acknowledgments

This research was supported by the National Natural Science Foundation of China (Nos. 81273426, 81430082, 81172974 and 31200694), the Fundamental Research Funds for the Central Universities (YD2014SK0002), Ph.D. Programs Foundation of Ministry of Education of China (20120096110007), Scientific Innovation Research of College Graduate in Jiangsu Province (KYLX_0624) and A Project Funded by the Priority Academic Program Development of Jiangsu Higher Education Institutions.

Appendix A. Supplementary data

Supplementary data associated with this article can be found, in the online version, at http://dx.doi.org/10.1016/j.bbrc.2014.10.149.

References

[1] G. Hannig, S.C. Makrides, Strategies for optimizing heterologous protein expression in *Escherichia coli*, Trends Biotechnol. 16 (1998) 54–60.
[2] S. Jana, J.K. Deb, Strategies for efficient production of heterologous proteins in *Escherichia coli*, Appl. Microbiol. Biotechnol. 67 (2005) 289–298.
[3] S. Kimura, T. Umemura, T. Iyanagi, Two-cistronic expression plasmids for high-level gene expression in *Escherichia coli* preventing translational initiation inhibition caused by the intramolecular local secondary structure of mRNA, J. Biochem. 137 (2005) 523–533.
[4] G. Georgiou, Expression of proteins in bacteria, protein engineering: principles and practice, Wiley-Liss Inc, New York, NY, 1996. 101–126.
[5] L. Gold, Expression of heterologous proteins in *Escherichia coli*, Methods Enzymol. 185 (1990) 11–14.
[6] S.C. Makrides, Strategies for achieving high-level expression of genes in *Escherichia coli*, Microbiol. Rev. 60 (1996) 512–538.
[7] G. Kudla, A.W. Murray, D. Tollervey, J.B. Plotkin, Coding-sequence determinants of gene expression in *Escherichia coli*, Science 324 (2009) 255–258.
[8] S. Kimura, T. Iyanagi, High-level expression of porcine liver cytochrome P-450 reductase catalytic domain in *Escherichia coli* by modulating the predicted local secondary structure of mRNA, J. Biochem. 134 (2003) 403–413.

[9] C. Bai, X. Wang, J. Zhang, A. Sun, D. Wei, S. Yang, Optimisation of the mRNA secondary structure to improve the expression of interleukin-24 (IL-24) in *Escherichia coli*, Biotechnol. Lett. (2014) 1–6.
[10] D. Hartz, D.S. McPheeters, L. Gold, Influence of mRNA determinants on translation initiation in *Escherichia coli*, J. Mol. Biol. 218 (1991) 83–97.
[11] X. Wu, H. Jörnvall, K.D. Berndt, U. Oppermann, Codon optimization reveals critical factors for high level expression of two rare codon genes in *Escherichia coli*: RNA stability and secondary structure but not tRNA abundance, Biochem. Biophys. Res. Commun. 313 (2004) 89–96.
[12] M. Tsukuda, K. Miyazaki, Directed evolution study unveiling key sequence factors that affect translation efficiency in *Escherichia coli*, J. Biosci. Bioeng. 116 (2013) 540–545.
[13] M.H. de Smit, J. Van Duin, Secondary structure of the ribosome binding site determines translational efficiency: a quantitative analysis, Proc. Natl. Acad. Sci. U.S.A. 87 (1990) 7668–7672.
[14] H. Wu, J. Pei, G. Wu, W. Shao, Overexpression of GH10 endoxylanase XynB from *Thermotoga maritima* in *Escherichia coli* by a novel vector with potential for industrial application, Enzyme Microb. Technol. 42 (2008) 230–234.
[15] S.W. Seo, J. Yang, G.Y. Jung, Quantitative correlation between mRNA secondary structure around the region downstream of the initiation codon and translational efficiency in *Escherichia coli*, Biotechnol. Bioeng. 104 (2009) 611–616.
[16] M.Z. Ladjemi, W. Jacot, T. Chardès, A. Pèlegrin, I. Navarro-Teulon, Anti-HER2 vaccines: new prospects for breast cancer therapy, Cancer Immunol. Immunother. 59 (2010) 1295–1312.
[17] R. Lorenz, S.H. Bernhart, C.H. Zu Siederdissen, H. Tafer, C. Flamm, P.F. Stadler, I.L. Hofacker, ViennaRNA Package 2.0, Algorithms Mol. Biol. 6 (2011) 26.
[18] J. Sambrook, E.F. Fritsch, T. Maniatis, Molecular cloning, Cold spring harbor laboratory press, New York, 1989.
[19] P. Balbas, F. Bolivar, Design and construction of expression plasmid vectors in *Escherichia coli*, Methods Enzymol. 185 (1990) 14–37.
[20] A. Das, Overproduction of proteins in *Escherichia coli*: vectors, hosts, and strategies, Methods Enzymol. 182 (1990) 93–112.
[21] S.M. Studer, S. Joseph, Unfolding of mRNA secondary structure by the bacterial translation initiation complex, Mol. Cell 22 (2006) 105–115.
[22] J.A. Steitz, K. Jakes, How ribosomes select initiator regions in mRNA: base pair formation between the 3′terminus of 16S rRNA and the mRNA during initiation of protein synthesis in *Escherichia coli*, Proc. Natl. Acad. Sci. U.S.A. 72 (1975) 4734–4738.
[23] L. Tang, R. Jiang, K. Zheng, X. Zhu, Enhancing the recombinant protein expression of halohydrin dehalogenase HheA in *Escherichia coli* by applying a codon optimization strategy, Enzyme Microb. Technol. 49 (2011) 395–401.
[24] K.M. Madduri, E.M. Snodderley, Expression of phosphinothricin *N*-acetyltransferase in *Escherichia coli* and *Pseudomonas fluorescens*: influence of mRNA secondary structure, host, and other physiological conditions, Protein Expression Purif. 55 (2007) 352–360.
[25] Y.S. Park, S.W. Seo, S. Hwang, H.S. Chu, J.-H. Ahn, T.-W. Kim, D.-M. Kim, G.Y. Jung, Design of 5′-untranslated region variants for tunable expression in *Escherichia coli*, Biochem. Biophys. Res. Commun. 356 (2007) 136–141.
[26] S.W. Seo, J.-S. Yang, H.-S. Cho, J. Yang, S.C. Kim, J.M. Park, S. Kim, G.Y. Jung, Predictive combinatorial design of mRNA translation initiation regions for systematic optimization of gene expression levels, Sci. Rep. 4 (2014).
[27] C.M. Arraiano, J.M. Andrade, S. Domingues, I.B. Guinote, M. Malecki, R.G. Matos, R.N. Moreira, V. Pobre, F.P. Reis, M. Saramago, The critical role of RNA processing and degradation in the control of gene expression, FEMS Microbiol. Rev. 34 (2010) 883–923.
[28] J.G. Belasco, MRNA degradation in prokaryotic cells: an overview, Academic Press, New York, 1993.
[29] W. Zhang, W. Xiao, H. Wei, J. Zhang, Z. Tian, MRNA secondary structure at start AUG codon is a key limiting factor for human protein expression in *Escherichia coli*, Biochem. Biophys. Res. Commun. 349 (2006) 69–78.